ROYAL SOCIETY OPEN SCIENCE

royalsocietypublishing.org/journal/rsos

Research

Cite this article: Hoa NT, Van Bay M, Mechler A, Vo QV. 2022 Theoretical insights into the antiradical activity and copper-catalysed oxidative damage of mexidol in the physiological environment. *R. Soc. Open Sci.* **9**: 211239. https://doi.org/10.1098/rsos.211239

Received: 23 October 2021
Accepted: 3 December 2021

Subject Category:
Chemistry

Subject Areas:
computational chemistry/medicinal chemistry

Keywords:
mexidol, emoxypine, density functional theory study, antiradical activity, antioxidants

Author for correspondence:
Quan V. Vo
e-mail: vvquan@ute.udn.vn

Downloaded from https://royalsocietypublishing.org/ on 14 March 2022

This article has been edited by the Royal Society of Chemistry, including the commissioning, peer review process and editorial aspects up to the point of acceptance.

ROYAL SOCIETY OF CHEMISTRY

THE ROYAL SOCIETY PUBLISHING

Theoretical insights into the antiradical activity and copper-catalysed oxidative damage of mexidol in the physiological environment

Nguyen Thi Hoa[1], Mai Van Bay[2], Adam Mechler[3] and Quan V. Vo[1]

[1]The University of Danang, University of Technology and Education, Danang 550000, Vietnam
[2]Department of Chemistry, The University of Danang, University of Science and Education, Danang 550000, Vietnam
[3]Department of Chemistry and Physics, La Trobe University, Victoria 3086, Australia

QVV, 0000-0001-7189-9584

Mexidol (**MD**, 2-ethyl-6-methyl-3-hydroxypyridine) is a registered therapeutic agent for the treatment of anxiety disorders. The chemical structure suggests that **MD** may also act as an antioxidant. In this study, the hydroperoxyl radical scavenging activity of **MD** was studied to establish baseline antioxidant activity, followed by an investigation of the effect of **MD** on the copper-catalysed oxidative damage in biological systems, using computational methods. It was found that **MD** exhibits moderate radical scavenging activity against $HOO^{\bullet}$ in water and pentyl ethanoate solvents following the single electron transfer and formal hydrogen transfer mechanisms, respectively. **MD** can chelate Cu(II), forming complexes that are much harder to reduce than free Cu(II): **MD** chelation completely quenches the Cu(II) reduction by ascorbic acid and suppresses the rate of reduction reaction by $O_2^{\bullet-}$ that are the main reductants of Cu(II) in biological environments. Therefore, **MD** exerts its anti-$HO^{\bullet}$ activity primarily as an OIL-1 inhibitor.

1. Introduction

Mexidol (**MD**, emoxypine, 2-ethyl-6-methyl-3-hydroxypyridine) is a drug used primarily for the treatment of anxiety. It is known to have antiischemic, antihypoxic, neuroprotective, antistress, nootropic and geroprotective properties [1,2]. **MD** is also used as an antioxidant for reducing tissue damage by reactive oxygen species [1,3]. For this reason, the radical

© 2022 The Authors. Published by the Royal Society under the terms of the Creative Commons Attribution License http://creativecommons.org/licenses/by/4.0/, which permits unrestricted use, provided the original author and source are credited.

Downloaded from https://royalsocietypublishing.org/ on 14 March 2022

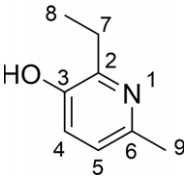

mexidol (**MD**)

Figure 1. Molecular structure and atomic numbering of mexidol (**MD**).

scavenging activity of **MD** was assessed in experimental studies [3,4]. The rate constant of **MD** reaction with peroxyl radical in methyl oleate was measured as $k = 2.8 \times 10^4\ M^{-1}\ s^{-1}$ [4], while that for 1,4-dioxane solvent was $k = 2.1 \pm 0.3 \times 10^4\ M^{-1}\ s^{-1}$ [3]. However, organic solutions such as methyl oleate and 1,4-dioxane are not suitable model environments to assess *in vivo* activity; in the physiologically relevant aqueous environment **MD** may exhibit very different behaviour due to dissociation of the OH moiety. Thus there is an impetus to study the antiradical activity of **MD** in physiological media.

In evaluating the antioxidant activity of **MD**, one has to also consider that pyridines are very good coordinating ligands and therefore it is highly likely that **MD** forms chelates with trace metals [5,6]. Previous studies showed that the presence of transition metals such as Cu(I) can produce hydroxyl radicals via the Fenton-like reaction (1.1) [7–11]:

$$Cu^{+} + H_2O_2 \rightarrow Cu^{2+} + HO^{\bullet}. \tag{1.1}$$

However, Cu(I) is not the most stable or abundant form of copper in physiological environments. The concentration of Cu(I) is defined by the amount of Cu(II) ions undergoing reduction by hyperoxide radical ($O_2^{\bullet -}$) or deprotonated ascobic acid (AA^-) with the rate constants $k = 4.46 \times 10^9\ M^{-1}\ s^{-1}$ and $1.33 \times 10^8\ M^{-1}\ s^{-1}$, respectively [10]:

$$Cu^{2+} + O_2^{\bullet -} \rightarrow Cu^{+} + {}^3O_2 \tag{1.2}$$

and

$$Cu^{2+} + AA^{-} \rightarrow Cu^{+} + AA^{\bullet}. \tag{1.3}$$

Chelation of Cu(II) has the potential to inhibit or suppress reactions (1.2) and (1.3) and therefore indirectly inhibit reaction (1.1). Thus, the capacity of **MD** to inhibit Cu(II) reduction by chelation is also of interest (figure 1).

Previous studies showed that computational method offers the most convenient path for studying structure–activity relationships in radical reactions to guide the design of novel antioxidants with enhanced activity [12–19]. In several prior studies, the radical scavenging activity of organic compounds in physiological environments was successfully evaluated by quantum chemistry calculations [20–23]. Thus, in this study, the $HOO^{\bullet}$ radical scavenging activity of **MD** was assessed in lipid and polar media using the quantum mechanics-based test for overall free radical scavenging activity (QM-ORSA) protocol [13,20]. Cu(II) chelation ability was also assessed and the ability of **MD** to act as an OIL-1 inhibitor of the copper-catalysed oxidative damage in biological systems was investigated.

2. Computational details

All density functional theory (DFT) calculations were carried out with Gaussian 09 suite of programs [24]. M06-2X functional [25] and 6-311++G(d,p) basis set were used for all calculations. The M06-2X functional is one of the most reliable methods to study thermodynamics and kinetics of radical reactions [20,25–30].

The stability of Cu(II) chelates was compared by calculating the Gibbs free energy of formation for all possible chelates that were first constructed with MD based on $[Cu(H_2O)_4]^{2+}$ geometry, optimized by molecular mechanics calculations using the Spartan software [31], then energy-minimized with DFT as per above.

The kinetic calculations were performed following the QM-ORSA protocol [13,20] and following the literature [29,30,32–37]. The details of the method are shown in electronic supplementary material, table S1. Atom-in-molecule (AIM) analysis [38] was performed by using the AIM2000 software [39].

Downloaded from https://royalsocietypublishing.org/ on 14 March 2022

3. Results and discussion

3.1. The HOO$^{\bullet}$ radical scavenging activity of **MD**

3.1.1. Gas phase evaluation

To reduce computing time, the radical scavenging activity of **MD** was first evaluated in the gas phase following the liturature [16,40], according to the three main reaction pathways: formal hydrogen transfer (FHT), single electron transfer followed by proton transfer (SETPT) and sequential proton loss electron transfer (SPLET) [41,42]. Radical adduct formation (RAF) is another common pathway that however requires a localized C=C bond; the aromatic ring of **MD** cannot support this mechanism [21,43,44]. The probabilities of the three feasible antioxidant mechanisms (FHT, SETPT and SPLET) were first evaluated by computing the main thermodynamic parameters associated with these mechanisms: bond dissociation enthalpy (BDE), ionization energy (IE) and proton affinity (PA), respectively. The calculated BDE, IE and PA values of **MD** are shown in electronic supplementary material, table S3.

The lowest BDE value was calculated for O3–H at 84.4 kcal mol^{-1}. This value is higher than that of natural antioxidants such as resveratrol (83.9 kcal mol^{-1}) [45], piceatannol (73.1 [21] or 75.1 [46] kcal mol^{-1}), Trolox (73.0 kcal mol^{-1}) [47] and ascorbic acid (73.9 kcal mol^{-1}) [47]. The BDE values of the C–H bonds are even higher by about 2.0–16.0 kcal mol^{-1}. At the same time, the IE and PA values are about 2.3 and 4.1 times higher than the lowest BDE value. Thus, based on the computed data, the antioxidant activity of **MD** in apolar and low-dielectric environments is projected to proceed via the FHT pathway. Calculations of $\Delta G°$ (Gibbs free energy change) values of the defining step of the **MD** + HOO$^{\bullet}$ reaction (electronic supplementary material, table S3) also confirmed that the FHT mechanism is the main path of the HOO$^{\bullet}$ radical scavenging activity of **MD** in the gas phase as well as in non-polar media.

Based on the thermodynamic results, the kinetics of the antiradical activity of **MD** was evaluated for the thermodynamically favourable positions and mechanisms according to the QM-ORSA protocol [20], and the data are shown in electronic supplementary material, table S4, and figure 2. The results suggest that the O3–H bond ($\Delta G^{\neq} = 13.0$ kcal mol^{-1}; $k_{Eck} = 2.95 \times 10^5$ M^{-1} s^{-1}; $\Gamma = 100.0\%$) is the only feasible site for H-abstraction during the **MD** + HOO$^{\bullet}$ reaction. The C–H bonds do not make any contribution ($\Gamma = 0\%$) in the overall rate constant of the antiradical activity of **MD**. That is consistent with the lowest BDE(O–H) values as calculated in the thermodynamic section. Thus the results suggest that the HOO$^{\bullet}$ radical scavenging activity of **MD** is dominated by the FHT mechanism at the O3–H bond; therefore, this reaction is further analysed in lipid medium.

3.1.2. The HOO$^{\bullet}$ radical scavenging activity of **MD** in physiological environments

In aqueous environment, the antiradical activity of acidic species is typically dominated by the ionic form [26,30,48]. Therefore, the protonation state of **MD** was first evaluated at physiological pH to find the most likely radical scavenging reactions. The **MD** structure allows protonation at the N1–H and O3–H bonds (figure 3); thus the pK_a values of **MD** were calculated based on the literature [48,49] and are shown in figure 3.

The calculated pK_a values for the amine were p$K_{a1} = 7.17$ (for N–H bond of cation form) and p$K_{a2} = 9.79$ (for O3–H bond). Therefore, in pH = 7.4 aqueous solution, **MD** exists in three states: the cation (H_2A^+, 37.0%), neutral (HA, 62.7%) and anion (A^-, 0.3%) states. Therefore, all three states were used in the kinetic evaluation of HOO$^{\bullet}$ radical removal of **MD** in water at physiological pH = 7.4.

The preferred radical scavenging pathways of the neutral and anionic states have been established; the cationic state requires initial evaluation. The computing of $\Delta G°$ of the H_2A^+ + HOO$^{\bullet}$ reaction for the possible pathways (electronic supplementary material, table S5) showed that the H_2A^+ + HOO$^{\bullet}$ reaction is only clearly spontaneous for FHT at the C7–H bond ($\Delta G° = -4.4$ kcal mol^{-1}). Thus this reaction was used to calculate the rate constant of the HOO$^{\bullet}$ radical scavenging of H_2A^+ in the aqueous solution. The overall rate constant of HOO$^{\bullet}$ + **MD** reaction was computed following equations (3.1) and (3.2); the results are presented in table 1 and figure 2.

In the lipid medium

$$k_{overall} = k_{app}\,(\mathrm{FHT(O3-H)-neutral}). \tag{3.1}$$

Downloaded from https://royalsocietypublishing.org/ on 14 March 2022

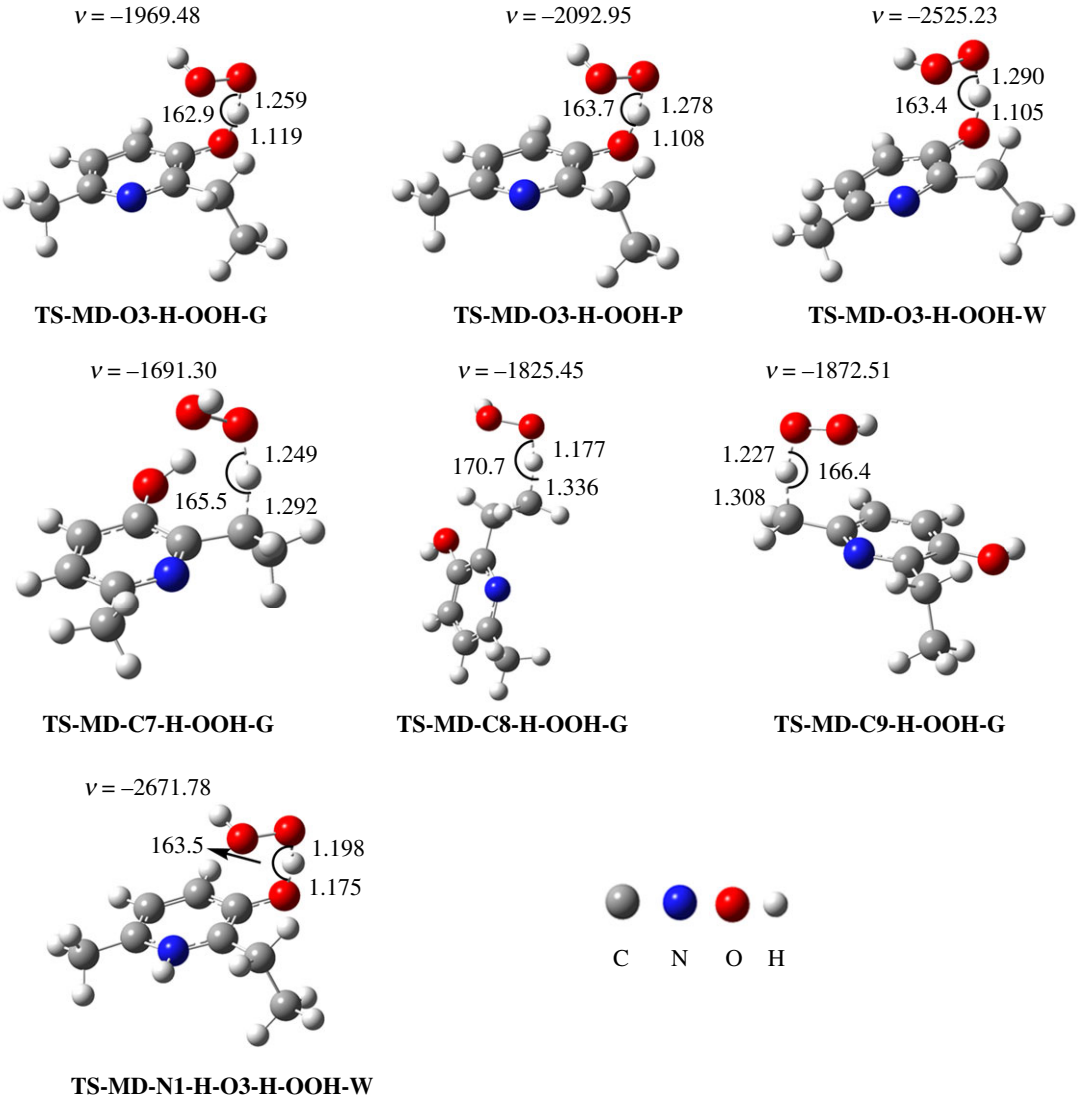

Figure 2. Optimized structures of the transition states (TS) along the FHT pathway of the HOO• radical scavenging activity of MD: (G) in the gas phase, (P) in pentyl ethanoate and (W) in water.

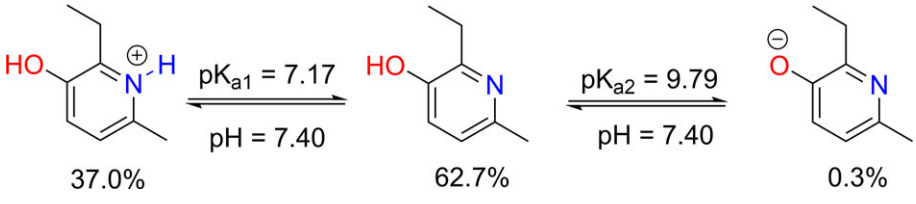

Figure 3. The deprotonation of **MD** at pH = 7.4.

In the aqueous solution

$$k_{\text{overall}} = k_f\,(\text{SET} - \text{HA}) + k_f\,(\text{SET} - \text{A}^-) + k_f\,(\text{FHT} - \text{H}_2\text{A}^+(\text{C7} - \text{H})) + k_f\,(\text{FHT} - \text{HA}(\text{O3} - \text{H})). \quad (3.2)$$

As per table 1, the HOO• + **MD** reaction in pentyl ethanoate is moderate with $k_{\text{overall}} = 4.40 \times 10^3\ \text{M}^{-1}\ \text{s}^{-1}$ by the FHT mechanism at the O3–H bond ($\Gamma = 100\%$). By contrast, **MD** exhibits good antiradical activity in water with $k_{\text{overall}} = 2.68 \times 10^4\ \text{M}^{-1}\ \text{s}^{-1}$. This reaction was defined ($\Gamma \sim 100\%$) by the SET pathway of the dianion A^-. The rate constant for the HA + HOO• reaction following the FHT mechanism at the O3–H bond is $k_f = 3.70 \times 10^3\ \text{M}^{-1}\ \text{s}^{-1}$ ($\Gamma = 13.8\%$), whereas that for the C7–H bond (H_2A^+) is only $k_f = 1.44 \times 10^{-3}\ \text{M}^{-1}\ \text{s}^{-1}$ and this reaction makes a negligible contribution (approx. 0%) to the total antiradical activity of **MD**. Compared with the reference antioxidant Trolox ($k = 1.30 \times 10^5$ and $1.00 \times 10^5\ \text{M}^{-1}\ \text{s}^{-1}$ in polar and

Downloaded from https://royalsocietypublishing.org/ on 14 March 2022

Table 1. Calculated $\Delta G^{\neq}$ (kcal mol^{-1}), κ, rate constants (k_{app}, k_f and $k_{overall}$ (M^{-1} s^{-1})), and Γ (%) in the **MD** + HOO$^{\bullet}$ reaction in the studied media.

		pentyl ethanoate				water					
mechanisms		$\Delta G^{\neq}$	κ	k_{app}	Γ	$\Delta G^{\neq}$	κ	k_{app}	f	k_f	Γ
SET	HA					36.8	18.1[a]	4.80×10^{-17}	0.627	3.01×10^{-17}	0.0
	A^-					5.1	16.0[a]	7.70×10^{6}	0.003	2.31×10^{4}	86.2
FHT	H_2A^+					24.4	483.1	3.90×10^{-3}	0.37	1.44×10^{-3}	0.0
	HA	15.9	328.1	4.80×10^{3}	100.0	16.6	1466.0	5.90×10^{3}	0.627	3.70×10^{3}	13.8
$k_{overall}$				4.80×10^{3}						2.68×10^{4}	

[a]The nuclear reorganization energy (λ, kcal mol^{-1}); $f = \%A^-/100$; $k_f = f \cdot k_{app}$; $\Gamma = k_f \cdot 100/k_{overall}$.

Downloaded from https://royalsocietypublishing.org/ on 14 March 2022

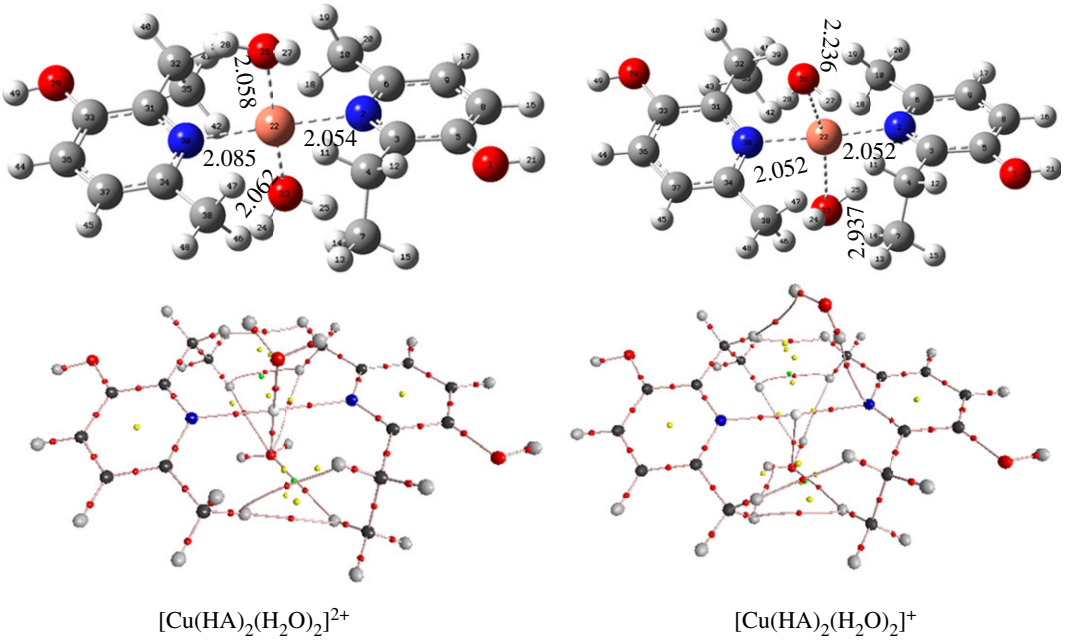

Figure 4. Optimized structures and AIM topological shapes of $[Cu(HA)_2(H_2O)_2]^{2+}$ and $[Cu(HA)_2(H_2O)_2]^{+}$ in aqueous solution, at 298.15 K. Small red spheres indicate bond critical points.

Table 2. The calculated $\Delta G°$, $\Delta G^{\neq}$, λ (kcal mol^{-1}), and rate constants (k_{app}, k_f and $k_{overall}$ (M^{-1} s^{-1})) at 298.15 K in the **MD** + Cu(II) reactions in water at pH = 7.40.

reactions	$\Delta G°$	$\Delta G^{\#}$	λ	k_{app}	f	k_f	$k_{overall}$
$H_2A^+ + Cu^{2+}$	39.6	94.7	5.3	2.20×10^{-57}	0.37	8.14×10^{-58}	2.19×10^{7}
$HA + Cu^{2+}$	20.5	28.7	6.2	6.00×10^{-9}	0.627	3.76×10^{-9}	
$A^- + Cu^{2+}$	−10.9	2.8	4.1	7.30×10^{9}	0.003	2.19×10^{7}	

nonpolar media, respectively) [40], the $HOO^{\bullet}$ radical scavenging activity of **MD** is lower in all of the studied environments. However, according to the empirical test for radical scavenging (activity should exceed 10^3) [20,50] **MD** can be considered an antioxidant, albeit a weak one.

3.2. OIL-1 inhibition of copper-catalysed oxidative damage in biological systems

It was first calculated whether **MD** in any form can reduce free Cu(II), i.e. whether the chelation itself is reductive or not. Results are shown in table 2. Only the anionic form yields a negative Gibbs free energy change and thus it may reduce Cu(II). However, in the catalytic cycle, it competes with $O_2^{\bullet -}$ and AA^- that have an order of magnitude higher rate constants (4.46×10^9 M^{-1} s^{-1} and 1.33×10^8 M^{-1} s^{-1}, respectively) [10]; hence **MD** does not contribute substantially to the reduction of free Cu(II).

To find the most stable complexes of the Cu(II) + **MD** reaction in water at pH = 7.4, the Cu(II) chelating ability of **MD** was evaluated considering the possible chelation sites of **MD** involving N and O atoms (electronic supplementary material, table S2). It was found that all of **MD** states (H_2A^+, HA and A^-) present in water could react with Cu(II) following 23 reactions and forming a range of complexes (electronic supplementary material, figure S1). The lowest Gibbs free energy of formation ($\Delta G°$, kcal mol^{-1}) was predicted for the complex $[Cu(HA)_2(H_2O)_2]^{2+}$ (reaction 14, *N* site, electronic supplementary material, table S2; figure 4) at −82.5 kcal mol^{-1} that is more than two times lower than the second lowest value (reaction 8, *N* site, electronic supplementary material, table S2). The equilibrium constant for reaction 14 is $K = 3.01 \times 10^{60}$ M^{-1} and this chelate will make up 100% of the possible complexes, based on Maxwell–Boltzmann calculations. The mono-, tri- and tetra-coordinate Cu–**MD** complexes were also investigated; however, these reactions were not favoured for the **MD** +

Downloaded from https://royalsocietypublishing.org/ on 14 March 2022

Table 3. Selected parameters at the BCPs at intermolecular contacts for $[Cu(HA)_2(H_2O)_2]^{2+}$ and $[Cu(HA)_2(H_2O)_2]^{+}$ in aqueous solution, at 298.15 K.

contacts	$\rho(r)$ (au)	$\nabla^2\rho(r)$ (au)	$G(r)^{a)}$ (au)	$V(r)^{b)}$ (au)	$G(r)/\lvert V(r)\rvert$	$H(r)^{c)}$ (au)	$E_{HB}^{d)}$ (kcal mol^{-1})
$[Cu(HA)_2(H_2O)_2]^{2+}$							
N2 ··· Cu	0.0695	0.3124	0.0872	−0.0962	0.9057	−0.0091	−30.2
N30 ··· Cu	0.0745	0.3426	0.0959	−0.1061	0.9035	−0.0102	−33.3
O23 ··· Cu	0.0597	0.3479	0.0878	−0.0886	0.9908	−0.0008	−27.8
O25 ··· Cu	0.0603	0.3514	0.0887	−0.0895	0.9907	−0.0008	−28.1
$[Cu(HA)_2(H_2O)_2]^{+}$							
N2 ··· Cu	0.0753	0.3492	0.0999	−0.1125	0.8881	−0.0126	−35.3
N30 ··· Cu	0.0753	0.3494	0.0999	−0.1124	0.8886	−0.0125	−35.3
O23 ··· Cu	0.0112	0.0441	0.0101	−0.0092	1.0991	0.0009	−2.9

Table 4. Calculated $\Delta G°$, λ, $\Delta G^{\neq}$ (kcal mol^{-1}), and rate constants (k_{app}, k_f and $k_{overall}$ (M^{-1} s^{-1})) for the reduction of Cu(II) and the most likely Cu(II) chelates by $O_2^{\bullet -}$ and AA^- in aqueous solution, at 298.15 K. $k(Cu^{2+} + O_2^{\bullet -}) = 4.46 \times 10^9$ M^{-1} s^{-1}; $k(Cu^{2+} + AA^-) = 1.33 \times 10^8$ M^{-1} s^{-1} [9,10].

reactions	$\Delta G°$	$\Delta G^{\neq}$	λ	k_{app}	f	k_f	$k_{overall}$
$[Cu(HA)_2(H_2O)_2]^{2+} + O_2^{\bullet -}$	−10.5	4.6	36.2	2.10×10^9	0.9975[a]	2.10×10^9	2.10×10^9
$[Cu(HA)_2(H_2O)_2]^{2+} + AA^-$	14.6	16.9	31.5	2.80	0.9993[b]	2.80	2.80

[a] $f(O_2^{\bullet -})$.
[b] $f(AA^-)$.

Cu(II) in water as indicated by the higher values of $\Delta G°$ of formation, compared with the $[Cu(HA)_2(H_2O)_2]^{2+}$. Thus, the antioxidant activity calculations were performed for this chelate.

For a deeper understanding of the structure and stability of the complexes, AIM analysis was applied to $[Cu(HA)_2(H_2O)_2]^{2+}$ and $[Cu(HA)_2(H_2O)_2]^{+}$ in water. The topological shape and selected parameters at the bond critical points (BCPs) at metal–molecule contacts of the complexes are presented in figure 4 and table 3.

It can be observed that $[Cu(HA)_2(H_2O)_2]^{2+}$ is mainly stabilized by Cu(II) ··· O and Cu(II) ··· N contacts. That was affirmed by the existence of BCPs (red spheres) in the Cu(II)–O23, Cu(II)–O25, Cu(II)–N2 and Cu(II)–N30 electron densities. It can be inferred from table 3 that all of the Cu(II) ··· X (X = O, N) electron densities are partly covalent in nature as indicated by $\nabla^2\rho(r) > 0$, $G(r)/\lvert V(r)\rvert \leq 1$ and $H(r) \leq 0$ [51,52]. These contacts play a decisive role in the stability of the complex $[Cu(HA)_2(H_2O)_2]^{2+}$ with the significant negative values of E_{HD} (−27.8 to −33.3 kcal mol^{-1}).

On the other hand, the stability of Cu(I) complex ($[Cu(HA)_2(H_2O)_2]^{+}$) is defined by the Cu(I) ··· N2(30) electron fluxes ($\nabla^2\rho(r) = 0.3492(0.3494)$, $G(r)/\lvert V(r)\rvert = 0.8881(0.8886)$, $H(r) = -0.0126(-0.0125)$ and $E_{HD} = -35.3$ kcal mol^{-1}; table 3). The contact of Cu(I) ··· O23 (H_2O) is a weak interaction with $\nabla^2\rho(r) = 0.0441$, $G(r)/\lvert V(r)\rvert = 1.0991$, $H(r) = 0.0009$ and $E_{HD} = -2.9$ kcalmol^{-1}. Thus two H_2O molecules in the $[Cu(HA)_2(H_2O)_2]^{+}$ are only solvating the system. That is consistent with previous studies of the coordination numbers and geometries of Cu(II) and Cu(I) complexes [9,53].

To evaluate the capacity of **MD** to reduce the copper-induced oxidative stress following the OIL-1 process in water at pH = 7.4, reduction reactions of the most stable complex ($[Cu(HA)_2(H_2O)_2]^{2+}$) and free Cu(II) were evaluated against typical copper-reducing species ($O_2^{\bullet -}$ and ascorbic acid anion (AA^-)) and the results are shown in table 4. It was found that the rate constant of the reaction of $O_2^{\bullet -}$ with $[Cu(HA)_2(H_2O)_2]^{2+}$ is 2.10×10^9 M^{-1} s^{-1} that is about 2.1 times lower than that of the reduction of free Cu(II) in water ($k(Cu^{2+} + O_2^{\bullet -}) = 4.46 \times 10^9$ M^{-1} s^{-1}) [10]. However, complexation suppressed the rate constant of AA^--driven reduction of Cu(II) by about 10^8 times compared to free Cu(II). Based on the calculated data, **MD** is a good OIL-1 inhibitor of Cu(II)-catalysed oxidative stress.

Downloaded from https://royalsocietypublishing.org/ on 14 March 2022

4. Conclusion

The antioxidant activity of **MD** was investigated by evaluating the radical scavenging activity and the OIL-1 suppression of copper-catalysed oxidative damage in biological systems using computer calculations. It was found that **MD** exhibits moderate hydroperoxyl radical scavenging activity in both lipid and polar media. The antiradical activity in non-polar environments follows the FHT mechanism at the O3–H bond, whereas in aqueous solution, it follows the SET pathway of the anion state. Chelation with **MD** could suppress the Cu(II) reduction by $O_2^{\bullet-}$ and AA^- in aqueous environment. Thus **MD** is predominantly an OIL-1 antioxidant.

Data accessibility. All relevant necessary data to reproduce all results in the paper are within the main text, electronic supplementary material and the Dryad Digital Repository: https://doi.org/10.5061/dryad.bzkh18997.

Authors' contributions. N.T.H.: data curation, formal analysis, investigation, validation, visualization, writing—original draft; M.V.B.: data curation, formal analysis, investigation, validation, writing—original draft; A.M.: conceptualization, project administration, software, supervision, writing—review & editing; Q.V.V.: conceptualization, formal analysis, methodology, project administration, resources, software, supervision, validation, writing—original draft, writing—review & editing. All authors gave final approval for publication and agreed to be held accountable for the work performed therein.

Competing interests. We declare we have no competing interests.

Funding. This research is funded by the Vietnamese Ministry of Education and Training under project no. B2021-DNA-16.

References

1. Karmanova E, Chernikov A, Usacheva A, Bruskov V. 2020 Antioxidant and gene-protective properties of ethylmethylhydroxypyridine succinate (Mexidol) in X-ray irradiation. *Pharm. Chem. J.* **54**, 673–677. (doi:10.1007/s11094-020-02255-2)
2. Voronina T. 2016 Pioneer antioxidant neuroprotection. 20 years in clinical practice. *RMJ* **24**, 434–438.
3. Semikasheva O, Yakupova L, Borisov I, Safiullin R. 2021 Quantitative analysis of the antioxidant activity of mexidol. *Pharm. Chem. J.* **54**, 1282–1285. (doi:10.1007/s11094-021-02356-6)
4. Perevozkina M. 2006 Synergism of sulfur-containing phenol (SO-4) with mexidol, α-tocopherol, and phospholipids. *Pharm. Chem. J.* **40**, 441–447. (doi:10.1007/s11094-006-0148-x)
5. Tolan DA, Kashar TI, Yoshizawa K, El-Nahas AM. 2021 Synthesis, spectral characterization, density functional theory studies, and biological screening of some transition metal complexes of a novel hydrazide–hydrazone ligand of isonicotinic acid. *Appl. Organomet. Chem.* **35**, e6205. (doi:10.1002/aoc.6205)
6. Abe T, Kametani Y, Yoshizawa K, Shiota Y. 2021 Mechanistic Insights into the dicopper-complex-catalyzed hydroxylation of methane and benzene using nitric oxide: a DFT study. *Inorg. Chem.* **60**, 4599–4609. (doi:10.1021/acs.inorgchem.0c03558)
7. Pham AN, Xing G, Miller CJ, Waite TD. 2013 Fenton-like copper redox chemistry revisited: hydrogen peroxide and superoxide mediation of copper-catalyzed oxidant production. *J. Catal.* **301**, 54–64. (doi:10.1016/j.jcat.2013.01.025)
8. Kim J, Martinez F, Metcalfe I. 2007 The beneficial role of use of ultrasound in heterogeneous Fenton-like system over supported copper catalysts for degradation of p-chlorophenol. *Catal. Today* **124**, 224–231. (doi:10.1016/j.cattod.2007.03.040)
9. Castañeda-Arriaga R, Pérez-González A, Alvarez-Idaboy JR, Galano A. 2018 Role of purines on the copper-catalyzed oxidative damage in biological systems: protection versus promotion. *Int. J. Quantum Chem.* **118**, e25527. (doi:10.1002/qua.25527)
10. Pérez-González A, Prejanò M, Russo N, Marino T, Galano A. 2020 Capsaicin, a powerful •OH-inactivating ligand. *Antioxidants* **9**, 1247. (doi:10.3390/antiox9121247)
11. Dempsey CE, Mason PE, Jungwirth P. 2011 Complex ion effects on polypeptide conformational stability: chloride and sulfate salts of guanidinium and tetrapropylammonium. *J. Am. Chem. Soc.* **133**, 7300–7303. (doi:10.1021/ja201349g)
12. Wright JS, Johnson ER, DiLabio GA. 2001 Predicting the activity of phenolic antioxidants: theoretical method, analysis of substituent effects, and application to major families of antioxidants. *J. Am. Chem. Soc.* **123**, 1173–1183. (doi:10.1021/ja002455u)
13. Galano A, Raúl Alvarez-Idaboy J. 2019 Computational strategies for predicting free radical scavengers' protection against oxidative stress: where are we and what might follow? *Int. J. Quantum Chem.* **119**, e25665. (doi:10.1002/qua.25665)
14. Abdel-Rahman MA, Al-Hashimi N, Shibl MF, Yoshizawa K, El-Nahas AM. 2019 Thermochemistry and kinetics of the thermal degradation of 2-methoxyethanol as possible biofuel additives. *Sci. Rep.* **9**, 4535. (doi:10.1038/s41598-019-40890-2)
15. Mahyuddin MH, Shiota Y, Yoshizawa K. 2019 Methane selective oxidation to methanol by metal-exchanged zeolites: a review of active sites and their reactivity. *Catal. Sci. Technol.* **9**, 1744–1768. (doi:10.1039/C8CY02414F)
16. Vo QV, Gon TV, Bay MV, Mechler A. 2019 Antioxidant activities of monosubstituted indolinonic hydroxylamines: a thermodynamic and kinetic study. *J. Phys. Chem. B* **123**, 10 672–10 679. (doi:10.1021/acs.jpcb.9b08912)
17. Leopoldini M, Russo N, Toscano M. 2011 The molecular basis of working mechanism of natural polyphenolic antioxidants. *Food Chem.* **125**, 288–306. (doi:10.1016/j.foodchem.2010.08.012)
18. Ghosh D, Acharya A, Tiwari SC, Krylov AI. 2012 Toward understanding the redox properties of model chromophores from the green fluorescent protein family: an interplay between conjugation, resonance stabilization, and solvent effects. *J. Phys. Chem. B* **116**, 12 398–12 405. (doi:10.1021/jp305022t)
19. Solntsev KM, Ghosh D, Amador A, Josowicz M, Krylov AI. 2011 What drives the redox properties of model green fluorescence protein chromophores? *J. Phys. Chem. Lett.* **2**, 2593–2597. (doi:10.1021/jz2011397)
20. Galano A, Alvarez-Idaboy JR. 2013 A computational methodology for accurate predictions of rate constants in solution: application to the assessment of primary antioxidant activity. *J. Comput. Chem.* **34**, 2430–2445. (doi:10.1002/jcc.23409)
21. Vo QV, Nam PC, Van Bay M, Thong NM, Mechler A. 2019 A theoretical study of the radical scavenging activity of natural stilbenes. *RSC Adv.* **9**, 42 020–42 028. (doi:10.1039/C9RA08381B)
22. Galano A, Mazzone G, Alvarez-Diduk R, Marino T, Alvarez-Idaboy JR, Russo N. 2016 Food antioxidants: chemical insights at the molecular

Downloaded from https://royalsocietypublishing.org/ on 14 March 2022

level. *Annu. Rev. Food Sci. Technol.* **7**, 335–352. (doi:10.1146/annurev-food-041715-033206)

23. Leopoldini M, Russo N, Chiodo S, Toscano M. 2006 Iron chelation by the powerful antioxidant flavonoid quercetin. *J. Agric. Food Chem.* **54**, 6343–6351. (doi:10.1021/jf060986h)
24. Frisch MJ *et al.* 2009 *Gaussian 09*. Wallingford, CT: Gaussian, Inc.
25. Zhao Y, Truhlar DG. 2008 How well can new-generation density functionals describe the energetics of bond-dissociation reactions producing radicals? *J. Phys. Chem. A* **112**, 1095–1099. (doi:10.1021/jp7109127)
26. Galano A, Alvarez-Idaboy JR. 2014 Kinetics of radical-molecule reactions in aqueous solution: a benchmark study of the performance of density functional methods. *J. Comput. Chem.* **35**, 2019–2026. (doi:10.1002/jcc.23715)
27. Alvarez-Idaboy JR, Galano A. 2012 On the chemical repair of DNA radicals by glutathione: hydrogen vs electron transfer. *J. Phys. Chem. B* **116**, 9316–9325. (doi:10.1021/jp303116n)
28. Alberto ME, Russo N, Grand A, Galano A. 2013 A physicochemical examination of the free radical scavenging activity of Trolox: mechanism, kinetics and influence of the environment. *Phys. Chem. Chem. Phys.* **15**, 4642–4650. (doi:10.1039/c3cp43319f)
29. Dzib E, Cabellos JL, Ortíz-Chi F, Pan S, Galano A, Merino G. 2019 *Eyringpy*: a program for computing rate constants in the gas phase and in solution. *Int. J. Quantum Chem.* **119**, e25686. (doi:10.1002/qua.25686)
30. Vo QV, Bay MV, Nam PC, Quang DT, Flavel M, Hoa NT, Mechler A. 2020 Theoretical and experimental studies of the antioxidant and antinitrosant activity of syringic acid. *J. Org. Chem.* **85**, 15 514–15 520. (doi:10.1021/acs.joc.0c02258)
31. Hehre W, Yu J, Klunzinger P, Lou L. 2000 *Spartan software*. Irvine, CA: Wavefunction Inc.
32. Evans MG, Polanyi M. 1935 Some applications of the transition state method to the calculation of reaction velocities, especially in solution. *Trans. Faraday Soc.* **31**, 875–894. (doi:10.1039/tf9353100875)
33. Eyring H. 1935 The activated complex in chemical reactions. *J. Chem. Phys.* **3**, 107–115. (doi:10.1063/1.1749604)
34. Truhlar DG, Hase WL, Hynes JT. 1983 Current status of transition-state theory. *J. Phys. Chem.* **87**, 2664–2682. (doi:10.1021/j100238a003)
35. Furuncuoglu T, Ugur I, Degirmenci I, Aviyente V. 2010 Role of chain transfer agents in free radical polymerization kinetics. *Macromolecules* **43**, 1823–1835. (doi:10.1021/ma902803p)
36. Vélez E, Quijano J, Notario R, Pabón E, Murillo J, Leal J, Zapata E, Alarcón G. 2009 A computational study of stereospecifity in the thermal elimination reaction of menthyl benzoate in the gas phase. *J. Phys. Org. Chem.* **22**, 971–977. (doi:10.1002/poc.1547)
37. Dzib E, Cabellos JL, Ortiz-Chi F, Pan S, Galano A, Merino G. 2018 Eyringpy 1.0.2, Cinvestav, Mérida, Yucatán.
38. Bader RF. 1991 A quantum theory of molecular structure and its applications. *Chem. Rev.* **91**, 893–928. (doi:10.1021/cr00005a013)
39. Biegler-König F. 2000 Journal, AIM 2000, University of Applied Sciences, Bielefeld, Germany.
40. Vo QV, Thong NM, Le Huyen T, Nam PC, Tam NM, Hoa NT, Mechler A. 2020 A thermodynamic and kinetic study of the antioxidant activity of natural hydroanthraquinones. *RSC Adv.* **10**, 20 089–20 097. (doi:10.1039/D0RA04013D)
41. Galano A. 2015 Free radicals induced oxidative stress at a molecular level: the current status, challenges and perspectives of computational chemistry based protocols. *J. Mex. Chem. Soc.* **59**, 231–262. (doi:10.29356/jmcs.v59i4.81))
42. Zheng Y-Z, Deng G, Liang Q, Chen D-F, Guo R, Lai R-C. 2017 Ror2 signaling regulates Golgi structure and transport through IFT20 for tumor invasiveness. *Sci. Rep.* **7**, 1. (doi:10.1038/s41598-016-0028-x)
43. Iuga C, Alvarez-Idaboy JR, Russo N. 2012 Antioxidant activity of*trans*-Resveratrol toward hydroxyl and hydroperoxyl radicals: a quantum chemical and computational kinetics study. *J. Org. Chem.* **77**, 3868–3877. (doi:10.1021/jo3002134)
44. Cordova-Gomez M, Galano A, Alvarez-Idaboy JR. 2013 Piceatannol, a better peroxyl radical scavenger than resveratrol. *RSC Adv.* **3**, 20 209–20 218. (doi:10.1039/c3ra42923g)
45. Shang Y, Zhou H, Li X, Zhou J, Chen K. 2019 Theoretical studies on the antioxidant activity of viniferifuran. *New J. Chem.* **43**, 15 736–15 742. (doi:10.1039/C9NJ02735A)
46. Zheng Y-Z, Chen D-F, Deng G, Guo R, Fu Z-M. 2018 The antioxidative activity of piceatannol and its different derivatives: antioxidative mechanism analysis. *Phytochemistry* **156**, 184–192. (doi:10.1016/j.phytochem.2018.10.004)
47. Xue Y, Zheng Y, An L, Dou Y, Liu Y. 2014 Density functional theory study of the structure–antioxidant activity of polyphenolic deoxybenzoins. *Food Chem.* **151**, 198–206. (doi:10.1016/j.foodchem.2013.11.064)
48. Vo QV, Hoa NT, Nam PC, Quang DT, Mechler A. 2020 In silico evaluation of the radical scavenging mechanism of mactanamide. *ACS Omega* **5**, 24 106–24 110. (doi:10.1021/acsomega.0c03646)
49. Galano A *et al.* 2016 Empirically fitted parameters for calculating pK_a values with small deviations from experiments using a simple computational strategy. *J. Chem. Inf. Model.* **56**, 1714–1724. (doi:10.1021/acs.jcim.6b00310)
50. Itagaki S, Kurokawa T, Nakata C, Saito Y, Oikawa S, Kobayashi M, Hirano T, Iseki K. 2009 In vitro and in vivo antioxidant properties of ferulic acid: a comparative study with other natural oxidation inhibitors. *Food Chem.* **114**, 466–471. (doi:10.1016/j.foodchem.2008.09.073)
51. Khanh PN, Phan CTD, Ho DQ, Van Vo Q, Ngan VT, Nguyen MT, Trung NT. 2019 Insights into the cooperativity between multiple interactions of dimethyl sulfoxide with carbon dioxide and water. *J. Comput. Chem.* **40**, 464–474. (doi:10.1002/jcc.25732)
52. Rozas I, Alkorta I, Elguero J. 2000 Behavior of ylides containing N, O, and C atoms as hydrogen bond acceptors. *J. Am. Chem. Soc.* **122**, 11 154–11 161. (doi:10.1021/ja0017864)
53. Fujii T, Moynier F, Abe M, Nemoto K, Albarède F. 2013 Copper isotope fractionation between aqueous compounds relevant to low temperature geochemistry and biology. *Geochim. Cosmochim. Acta* **110**, 29–44. (doi:10.1016/j.gca.2013.02.007)